Semi-automatic assessment of skin capillary density: Proof of principle and validation

Microvascular Research 90 (2013) 192–198

Contents lists available at ScienceDirect

Microvascular Research

journal homepage: www.elsevier.com/locate/ymvre

Semi-automatic assessment of skin capillary density: Proof of principle and validation

E.H.B.M. Gronenschild [a,1], D.M.J. Muris [b,1], M.T. Schram [b], Ü. Karaca [b], C.D.A. Stehouwer [b], A.J.H.M. Houben [b,*]

[a] Department of Psychiatry and Neuropsychology and School for Mental Health and Neuroscience (MeHNs), Maastricht University Medical Centre (MUMC), Maastricht, The Netherlands
[b] Department of Internal Medicine and Cardiovascular Research Institute Maastricht (CARIM), Maastricht University Medical Centre (MUMC), Maastricht, The Netherlands

ARTICLE INFO

Article history:
Accepted 14 August 2013
Available online 26 August 2013

ABSTRACT

Background: Skin capillary density and recruitment have been proven to be relevant measures of microvascular function. Unfortunately, the assessment of skin capillary density from movie files is very time-consuming, since this is done manually. This impedes the use of this technique in large-scale studies. We aimed to develop a (semi-) automated assessment of skin capillary density.
Methods: CapiAna (Capillary Analysis) is a newly developed semi-automatic image analysis application. The technique involves four steps: 1) movement correction, 2) selection of the frame range and positioning of the region of interest (ROI), 3) automatic detection of capillaries, and 4) manual correction of detected capillaries. To gain insight into the performance of the technique, skin capillary density was measured in twenty participants (ten women; mean age 56.2 [42–72] years). To investigate the agreement between CapiAna and the classic manual counting procedure, we used weighted Deming regression and Bland–Altman analyses. In addition, intra- and inter-observer coefficients of variation (CVs), and differences in analysis time were assessed.
Results: We found a good agreement between CapiAna and the classic manual method, with a Pearson's correlation coefficient (r) of 0.95 ($P < 0.001$) and a Deming regression coefficient of 1.01 (95%CI: 0.91; 1.10). In addition, we found no significant differences between the two methods, with an intercept of the Deming regression of 1.75 (−6.04; 9.54), while the Bland–Altman analysis showed a mean difference (bias) of 2.0 (−13.5; 18.4) capillaries/mm^2. The intra- and inter-observer CVs of CapiAna were 2.5% and 5.6% respectively, while for the classic manual counting procedure these were 3.2% and 7.2%, respectively. Finally, the analysis time for CapiAna ranged between 25 and 35 min versus 80 and 95 min for the manual counting procedure.
Conclusion: We have developed a semi-automatic image analysis application (CapiAna) for the assessment of skin capillary density, which agrees well with the classic manual counting procedure, is time-saving, and has a better reproducibility as compared to the classic manual counting procedure. As a result, the use of skin capillaroscopy is feasible in large-scale studies, which importantly extends the possibilities to perform microcirculation research in humans.

Introduction

It is increasingly being recognized that microvascular dysfunction may be a key feature in the development of both obesity-related hypertension and insulin resistance (Houben et al., 2012; Jonk et al., 2007; Muris et al., 2013). In fact, several studies have shown the relevance of microvascular effects of insulin (Jonk et al., 2010; Serne et al., 2002) and their role in whole body glucose uptake (Kubota et al., 2011; Meijer et al., 2012). The skin is a unique site allowing simple and reproducible assessment of capillary density and capillary recruitment. Specifically, the skin is the only site available in humans allowing direct, non-invasive visualization of capillaries at rest and during provocative stimuli. In addition, the cutaneous microcirculation is considered a representative vascular bed to examine generalized systemic microvascular dysfunction (Holowatz et al., 2008). Importantly, with regard to specific effects on insulin, several studies have demonstrated comparable metabolic (Lang, 1992) and vascular effects (Clerk et al., 2006; Meijer et al., 2012) of insulin in muscle and skin. Moreover, it has been demonstrated that the (systemic) effects of obesity and free fatty acids on insulin-mediated microvascular recruitment in muscle (Clerk et al., 2006; Liu et al., 2009) can be reproduced in skin (de Jongh et al., 2004a,b). These data strongly suggests that vascular responses observed in skin parallel those in muscle, and thus that measurement of the skin microvasculature is an important tool for the assessment of microvascular function.

Skin capillaroscopy is often used to study the skin microvasculature (Jonk et al., 2010; Serne et al., 1999). Unfortunately, the analysis of skin capillary density from movie files is done manually, and thus is very time-consuming. This impedes the use of this technique in large-scale

* Corresponding author at: Maastricht University Medical Centre, Department of Internal Medicine, P.O. Box 5800, 6202 AZ, Maastricht, The Netherlands.
E-mail address: b.houben@maastrichtuniversity.nl (A.J.H.M. Houben).
[1] Both authors contributed equally.

0026-2862/$ – see front matter © 2013 Elsevier Inc. All rights reserved.
http://dx.doi.org/10.1016/j.mvr.2013.08.003

investigations. Hence, an automated assessment of skin capillary density would facilitate the use of capillary microscopy in larger studies.

We developed a semi-automatic method for the assessment of skin capillary density, i.e., an image analysis application named CapiAna (Capillary Analysis). The purpose of this report is to describe this new technique and to present accuracy, reproducibility and efficiency results.

Materials and methods

Subjects

Twenty Caucasian subjects (ten women; mean age 56.2 [42–72] years) participated in this study. These subjects were selected from the Maastricht Study (http://themaastrichtstudy.com), a large-scale cohort study. To ensure that we tested the agreement and reproducibility across a wide range of capillary densities, these subjects were selected based on their (baseline) skin capillary densities. All participants gave their informed consent. The Maastricht Study protocol was approved by the local ethics committee (NL31329.068.10) and was performed in accordance with the Declaration of Helsinki.

Skin capillaroscopy

Skin capillaroscopy was conducted after 30 min of acclimatization in a quiet, temperature-controlled (24 °C) room, with the subjects in supine position and the investigated hand at heart level. Measurements were performed after a 10 h fast and all subjects abstained from drinking alcohol and smoking for a period of 24 h and performing strenuous exercise for a period of 48 h. In the present study, skin capillaries were visualized in the skin of the dorsal phalanges of the third and fourth finger of the right hand by use of a digital video microscope (Capiscope®, KK Technology, Honiton UK, http://www.kktechnology.com/) with a system magnification of 100×. Capillaries were visualized ~4.5 mm proximal to the terminal row of capillaries in the middle of the nailfold, where capillaries run perpendicularly to the skin. In this visual field, the investigator selected a region of interest (ROI) of a square millimeter of skin. Subsequently, capillaries with eye-catching morphological features were kept on the same spot in the visual field (marked by a dot on the monitor) to ensure that capillary density was measured in exactly the same visual field during the entire experiment (Jonk et al., 2011a). Capillary density was measured under three conditions. First, we measured baseline capillary density, defined as the number of continuously erythrocyte-perfused capillaries per square millimeter of skin. Second, we used post-occlusive reactive hyperemia after 4 min of arterial occlusion to assess functional capillary reserve capacity (hyperemic capillary recruitment). For the assessment of reactive hyperemia, a miniature cuff (Digit cuff, Hokanson, Inc., Bellevue, WA, USA) was applied on the base of the investigated finger and inflated to suprasystolic pressure (~260 mm Hg). Third, we applied venous congestion, with the cuff inflated to 60 mm Hg for 2 min, to expose the maximal number of capillaries. Between conditions, a resting interval of 5 min was used.

Automatic method

CapiAna is a software application to detect capillaries semi-automatically in a sequence of uncompressed monochrome images (frames) captured by the Capiscope. It comprises a series of image processing steps which will be described in detail below. Only minimal user interaction is required.

Data acquisition

The Capiscope captures image data at a rate of 25 frames per second. Each frame measures 640 × 480 pixels with 256 gray levels per pixel. The uncompressed raw data were transferred to the PC for subsequent processing.

Determination of position shifts

The first step was the determination of the position shifts caused by the movements (mainly due to respiration) of the finger during image acquisition. We used a technique based on phase shifts in the Fourier domain, which was shown to be more accurate than for instance cross-correlation (Giele et al., 2001). For this purpose, within a centrally located square of 256 × 256 pixels, an edge enhancement filter (Prewitt) followed by a Fourier transformation was applied to each frame of the full frame sequence. In the Fourier domain, the phase shift image between each frame and the first frame was derived. The position of the maximum intensity corresponded to the position shift of each frame with respect to the first frame. Note that by this method, the position shifts were always derived in integer precision. The assessed sequence of position shifts for all frames was smoothed by a median filter, independently in the X and Y directions. This sequence was saved to disk for later use. If a position shift was found too large, the corresponding frame was marked invalid because it contained too much movement blurring. Such invalid frames were not taken into account in the subsequent analysis.

Frame range selection

By looping through the frame sequence, the user can inspect the quality and select manually the range of contiguous frames that will be used for the detection of the capillaries. The time duration of this episode was generally on the order of 16 s, corresponding to 400 frames.

ROI positioning

The second manual interaction was the positioning of a squared ROI measuring 1 × 1 mm (248 × 248 pixels). Its size in pixels was determined previously by calibration measurements using a ruler (resulting in a resolution of 4.03 μ per pixel). Only within this ROI will the detection take place. The position shifts derived in the previous step were applied to this ROI so that for each frame the same area was being analyzed, as if the ROI was fixed to the skin of the finger.

Detection of capillaries

The actual detection of the capillaries was data-driven and based on a combination of gray-level and morphological filtering, and took information of all the selected frames into account. There were several reasons for this approach. The images were far from being uniform in intensity (due to the positions of the LED lights fixed to the microscopic device), making techniques solely based on intensity thresholding rather useless. Furthermore, the fact that during baseline measurements some capillaries were not perfused continuously impeded the use of correlation techniques. Finally, the application of adaptive filtering techniques did not make sense because the shape of a capillary was not the same for all capillaries, both within a frame and between frames.

Because the number of capillaries present in each frame varied during time, we noted that splitting the selected frame range into N intervals of 100 frames each resulted in a more robust detection. The intervals were contiguous without any overlap, except for the last one in case the number of selected frames, NF, was not a multiple of 100. For each interval, k, so-called seed points were derived, as follows (Fig. 1). A minimum-intensity image was built from the frames after correction of the position shifts and high-pass filtered to remove the non-uniform background. Next, the resulting image was binarized between 0 and the median intensity and then morphologically dilated. This result was called $HPImage^k$, where superscript k refers to the k-th interval. In addition, a variance image was built from the frames, as follows. Each frame was corrected for the position shift and then a random position shift was applied to it. We used a uniformly random number generator (called "Random3" in Numerical Recipes in C (Press et al., 1989)) with an amplitude of 3 pixels, a value which was derived empirically to produce the best results. For each pixel, the variance in intensity through the 100 frames was computed. This variance image was binarized

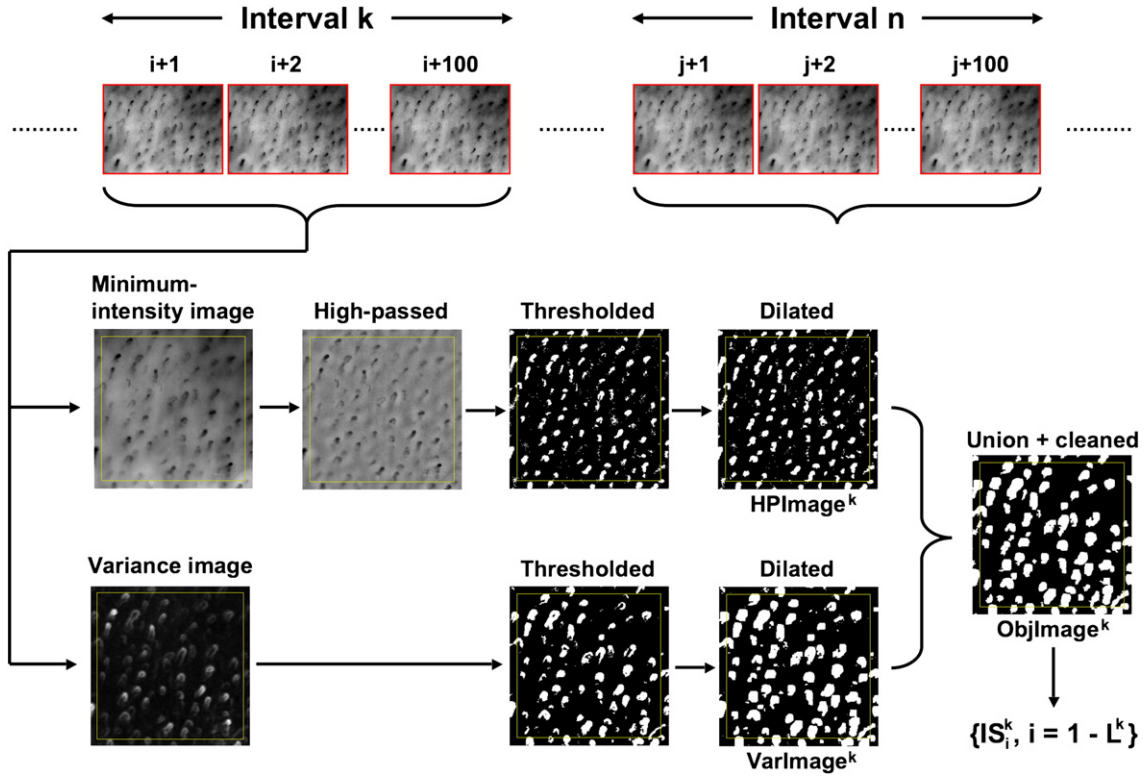

Fig. 1. Illustration of the procedure to derive the initial seed points (estimated positions of the capillaries). The selected *NF* frames were split into *N* contiguous intervals of 100 frames each. For each interval, a minimum-intensity image and variance image was derived and processed separately, resulting into binarized images, called HPImage^k and VarImage^k, respectively, where superscript *k* refers to the *k*-th interval. In these binarized images, so-called objects were present, where an object was defined as a set of linked (neighboring) white pixels. Both images were combined into a single image by retaining only the objects which were intersecting and by subsequently removing objects which were smaller than 10 pixels in size. The resulting image was called ObjImage^k and the set of initial seed points $\{IS_i^k, i = 1 - L^k\}$ was constituted by the top-left positions of all L^k objects inside the ROI (yellow rectangle). Note that for each interval a different set of initial seed points was derived.

between the 90 percentile and maximum intensity value and then morphologically dilated. This result was called VarImage^k. In both binarized images, objects could be identified where an object was defined as a set of linked (neighboring) white pixels. Finally, only the intersecting objects from both images were kept (called ObjImage^k) and objects smaller than 10 pixels were removed as these were considered spurious. The top-left position of each object within the squared ROI was determined and these positions constituted the set of initial seed points, $\{IS_i^k, i = 1 - L^k\}$. Note that all positions were corrected for position shifts. It was found that the combination of such a minimum-intensity image and variance image improved the robustness of the technique.

After processing all the *N* intervals of 100 frames in this way we ended up with *N* sets of initial seed points. Note that the number of seed points in each interval ($= L^k$) may differ. These sets of positions were merged and subsequently pruned, i.e., only positions that were different were kept. The result was a set of final seed positions, $\{S_i,\ i = 1 - NL\}$, with $NL = \left[\left(\sum_k L^k\right) - N_{eq}\right]$, where N_{eq} is the number of removed equal positions (Fig. 2). A seed point derived by this procedure represented an initial guess of the position of a capillary in all *NF* frames.

For each of the *N* intervals, a number of operations were needed to find out if a seed point really represented a capillary and to prevent multiple counting since seed points may be very near each other and thus referring to the same capillary. Of note, this additional processing was required only because the selected frame range was split into *N* subsequent intervals of 100 frames. First, it was checked if a seed point was located in one of the objects in ObjImage^k since a seed point derived in interval *n* may be different from a seed point derived in interval $m \neq n$. If so, then for each of the 100 frames in the *k*-th interval the position with the minimum intensity for pixels within this object was derived and added to the initial list of positions of capillaries (Fig. 3). If the above check failed, an invalid position was added for each of the pertaining 100 frames. After all the *N* intervals were processed, a two-dimensional list of initial positions, IP_{ij}, existed, all having a correspondence with one of the seed points. In other words, each seed point S_i was associated with a list of *NF* initial positions, $\{IP_{ij}, j = 1 - NF\}$. For each *i*, this list was smoothed by taking the average over all *NF* frames, excluding invalid positions. The result was a list of average positions, $\{AP_i, i = 1 - NL\}$ (Fig. 4).

Because seed points from different intervals were integrated and thus may be located close to each other, we had to make sure that each seed point would correspond to a unique final capillary. To this end, average positions which were close to each other were replaced

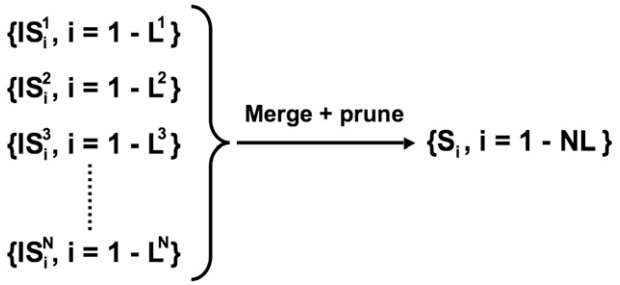

Fig. 2. The determination of the final set of seed points. The set of initial seed points $\{IS_i^k, i = 1 - L^k\}$ for each *k*-th interval ($k = 1 - N$) was combined into a single set and pruned, i.e., only positions that were different were kept.

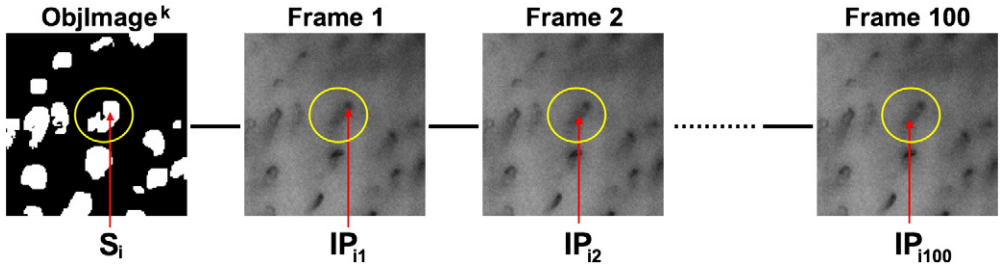

Fig. 3. The promotion of a final seed point S_i to an initial capillary position IP_{ij} in each of the 100 frames in the k-th interval. If a seed point was located in one of the objects in $ObjImage^k$ then the initial capillary position was set to the position of the minimum intensity of pixels within this object in each frame. If a seed point was not within any object then invalid positions were inserted instead. After processing all *N* intervals, each seed point was associated with *NF* initial capillary positions.

by their average, resulting in the final set of *NC* unique capillary positions, $\{P_i,\ i = 1 - NC\}$ (Fig. 4). For display purposes, this one-dimensional list was extended to a two-dimensional list ($NC \times NF$) by copying these positions to each frame and applying the position shifts.

Output

The final capillary positions were shown as crosses superimposed on the displayed frame in either green or red color, where green indicated that a capillary was detected in all frames (continuously perfused) and red if this was not the case (Fig. 5). Because of the fact that the positions were averaged over all frames and that to each position the position shift was added, the crosses moved in near synchrony with the movements of the finger during movie display of the frame sequence. The user is offered the ability to add or remove positions or to change green into red capillaries or vice versa, if necessary. All manual editing is indicated by a different appearance of a position on the monitor.

The positions and, in addition, a text file with a summary of the results can be saved to disk. This summary includes a list of the number of detected capillaries in each frame (also differentiated into green and red), and the total number of capillaries present in the whole frame sequence, differentiated into the different categories, such as green, red, manually added green or red, and manually changed from green into red.

Practical considerations

For our research, measurements were carried out typically during three different conditions: 1) baseline; 2) hyperemic capillary recruitment; and 3) venous congestion. To be able to properly analyze the data, it is important to position the square-mm ROI at the same location of the finger for each of the three corresponding measurements. This was done by making use of three instances of CapiAna. By minimizing and moving the three display windows next to each other on the monitor, it allowed easy identification of similar ROIs.

Semi-automatic and manual counting procedure

One single experienced investigator (D.M.J.M.) assessed capillary density of the three conditions (i.e., baseline capillary density, hyperemic capillary recruitment, and capillary density during venous congestion) with 1) the semi-automatic image analysis application (CapiAna) and 2) the classic manual counting procedure. The analysis time of both counting procedures was recorded.

For the semi-automatic counting procedure, we assessed the number of capillaries from a running movie file using CapiAna which involved four steps: 1) movement correction, 2) selection of the frame range and positioning of the ROI, 3) automatic detection of capillaries located in this ROI and frame range, and 4) manual correction of detected capillaries.

For the manual counting procedure, we manually counted the number of capillaries, which has been described in detail elsewhere (Jonk et al., 2011a; Serne et al., 1999). Briefly, capillaries were counted using the naked eye from a freeze-framed reproduction of the movie-file and from the running movie-file, when it was uncertain whether a capillary was present or not.

The investigator determined capillary density for the two methods at exactly the same frame range and ROI after a minimum of two weeks. The number of capillaries at baseline, directly after release of the cuff, and during venous congestion was counted for 16 s (i.e., 400 frames). The mean of both measurements at the two fingers was used for analyses.

Statistical analyses

Method comparison and agreement

We used the paired-sample *t*-test to study the differences in capillary density between the semi-automatic image analysis application (CapiAna) and the manual counting procedure. To investigate

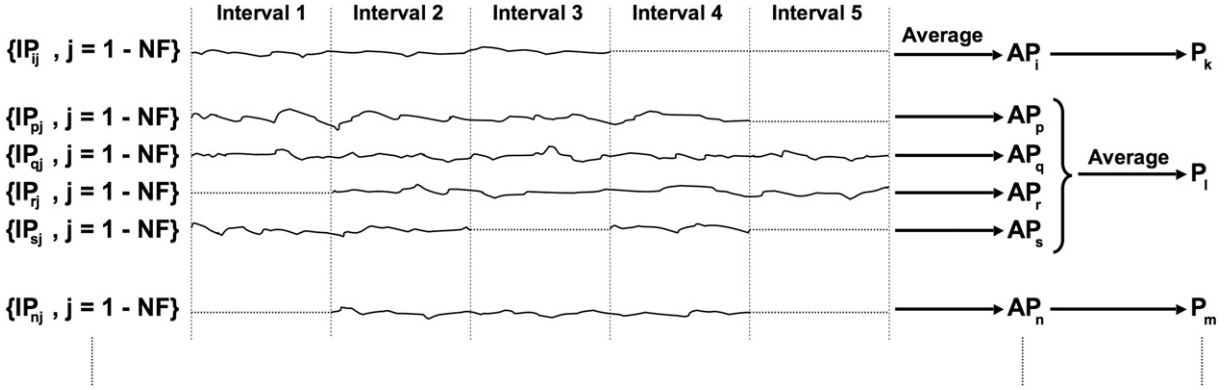

Fig. 4. The conversion of an initial to a final capillary position. The list of *NF* initial positions associated with seed point S_i was smoothed by taking the average AP_j. Because seed points could be located close together, so could the averaged positions. Therefore, averaged positions which were near each other were replaced by their average, e.g., the final capillary position P_l. In all other cases the final capillary position was taken equal to the averaged position, e.g., P_k and P_m. Note that for readability we have considered only 5 intervals to illustrate this process. Dashed lines indicate invalid positions (associated seed point was outside any object in ObjImage).

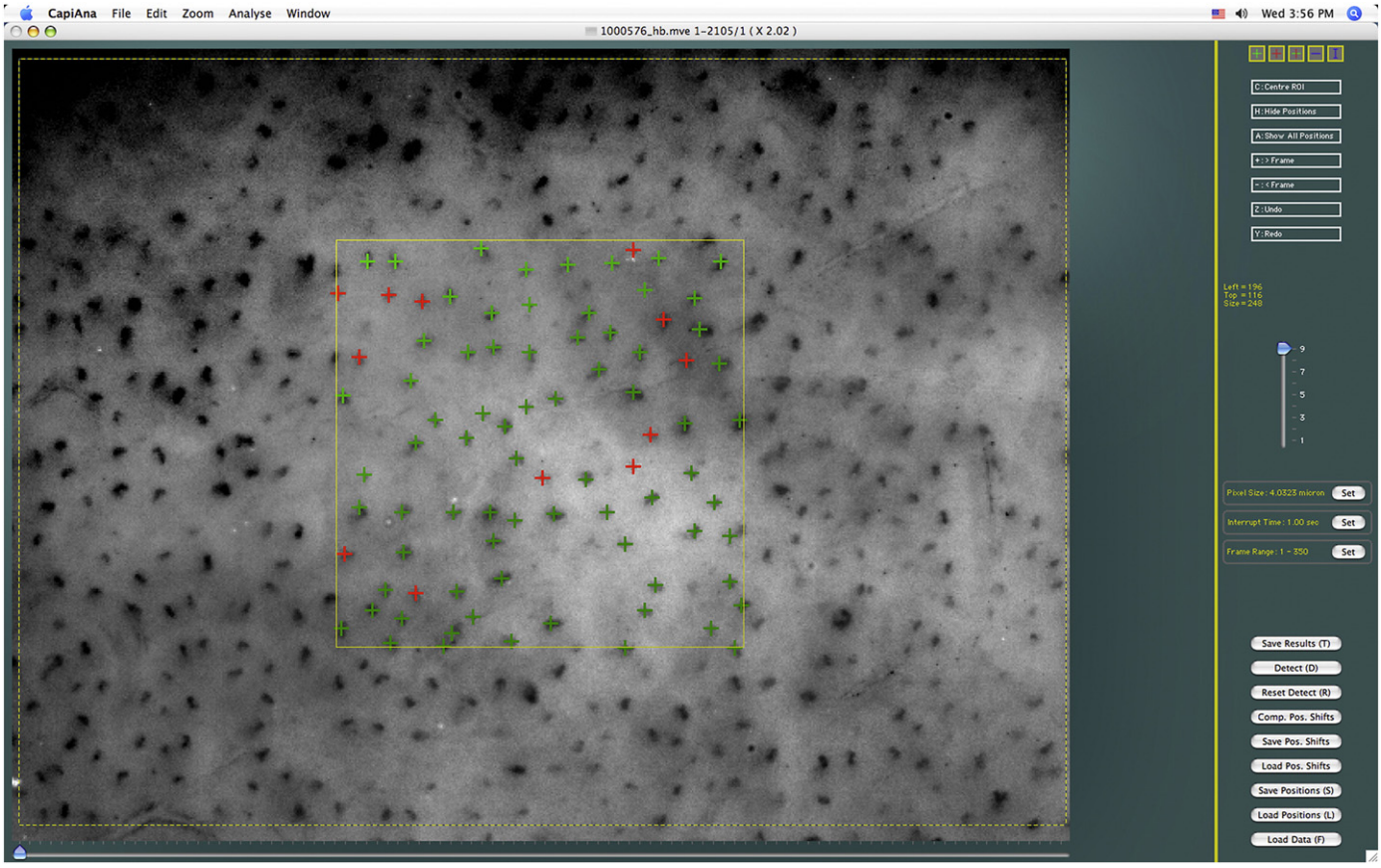

Fig. 5. Screenshot of the display window of CapiAna. The main part shows the captured contrast enhanced data. Superimposed are the results of the automatic detection of the capillaries. Green crosses denote capillaries which are detected in all selected frames, i.e., continuously perfused. Red crosses indicate intermittently perfused capillaries. The yellow rectangle represents the 1 × 1 mm ROI. The dashed yellow line shows the allowable area in which the ROI can be positioned such that it will never be outside the image borders due to the finger movements. At the bottom, a scrollbar is provided to be able to quickly navigate through the frames. At the right various tools and buttons are presented. For instance, the five small rectangles at the top are used for manual corrections. With the small scrollbar the user can change the frame rate at which the frames are displayed in movie mode. Also the frame range can be selected by pressing the lower "Set" button. Finally, the row of large buttons at the bottom enables the user to load and save data and results or to reset or start the detection.

agreement between the methods, capillary densities as determined by CapiAna and the manual counting procedure were compared by use of Pearson's correlation and weighted Deming regression. By the latter analysis, the regression coefficient and intercept between the methods were assessed (i.e., proportional bias and constant bias, respectively). When two methods produce equivalent results the regression coefficient will be one and the intercept will be zero, resulting in the equation $y = x$ (Martin, 2000). This statistical technique for method comparison is superior to simple linear regression by taking into account the error in both the dependent and independent variables (Martin, 2000; van Bussel et al., 2013). A Bland–Altman plot was used to investigate levels of agreement between the methods. We assessed the mean difference (bias) and 95%CI (limits of agreement) (Bland and Altman, 1986).

Reproducibility

To establish reproducibility, we calculated the intra- and inter-observer coefficients of variation (CV), defined as the SD divided by the mean of the differences, multiplied by 100. For the intra-observer CV, grader 1 (D.M.J.M.) counted the number of capillaries for the three conditions with CapiAna and repeated this semi-automatic counting procedure after a minimum of two weeks. For the inter-observer CV, a second experienced investigator (Ü.K., grader 2) counted the number of capillaries for the three conditions with CapiAna in exactly the same ROI and frame range as grader 1.

All analyses were performed with the use of the Statistical Package for Social Sciences (IBM, version 20.0, Chicago, Illinois, USA), except weighted Deming regression, which was analyzed using the Analyse-It software (Analyse-it Software Ltd., Leeds, UK) for Microsoft Excel (Microsoft Corporation, Washington, USA). A P-value < 0.05 was considered statistically significant.

Results

Table 1 shows the capillary densities as measured with CapiAna and the manual counting procedure. The capillary density during baseline, hyperemic (functional) capillary recruitment, and venous congestion did not significantly differ between CapiAna and the manual counting procedure, although baseline capillary density derived with CapiAna was borderline significantly ($P = 0.06$) higher as compared to the manual counting procedure.

Table 1
Capillary densities as determined by the semi-automatic image analysis application (CapiAna) and the manual procedure.

	Capillary density CapiAna	Capillary density manual counting procedure	Difference between methods	P-value
Baseline	67.5 ± 25.7	63.0 ± 22.6	4.5 (−9.3; 0.3)	0.06
Hyperemic (functional) capillary recruitment	87.4 ± 21.9	86.6 ± 22.9	0.9 (−4.3; 2.6)	0.61
Venous congestion	95.2 ± 24.4	93.3 ± 23.8	1.9 (−4.8; 1.0)	0.19

Data are means ± SD or means (lower and upper limit).
Capillary density based on the number of capillaries per square millimeter of finger skin.

We found a Pearson's correlation coefficient (r) of 0.95 ($P < 0.001$). The Deming regression coefficient was 1.01 (95%CI: 0.91; 1.10; $P = 0.86$) with an intercept of 1.75 (−6.04; 9.54; $P = 0.65$) (Fig. 6). In addition, the Bland–Altman analysis showed a mean difference (bias) of 2.0 (−13.5; 18.4) capillaries/mm^2 (Fig. 7). The results indicate that CapiAna and the classic manual method are in good agreement (i.e., the equation $y = 1.01x + 1.75$ was not significantly different from the equation $y = x$ (Fig. 6)) with no significant differences between the methods (Fig. 7).

The reproducibility of CapiAna is presented in Table 2. The semi-automatically derived capillary density for the three conditions was highly reproducible by the same rater with a CV of 2.5% (ranging from 1.7 to 3.5%). The inter-observer CV for the three conditions was 5.6% (ranging from 4.9 to 6.6%). In addition, intra- and inter-observer CVs for the manual counting procedure for the three conditions were 3.2% (ranging from 1.8 to 4.5%) and 7.2% (ranging from 6.8 to 8.0%) respectively as reported elsewhere (Jonk et al., 2011b).

The complete analysis time for CapiAna (i.e., assessment of capillary density of the three conditions for two fingers) ranged from 25 to 35 min, while for the manual counting procedure this ranged from 80 to 95 min.

Discussion

We have developed a semi-automatic image analysis application (CapiAna) for the assessment of skin capillary density, which 1) is in agreement with the manual counting procedure; 2) has a better reproducibility as compared to the manual counting procedure and 3) is intrinsically faster as compared to the manual counting procedure, with time savings of approximately 60 min per subject. As a result, skin capillaroscopy can be more easily applied in large-scale studies.

The automatic detection steps of CapiAna may potentially introduce systematic errors. Firstly, once a seed point is located in one of the objects then this is promoted to a capillary in all the corresponding 100 frames, irrespective of the presence or absence of a capillary. This may generate false-positive detections. Indeed, the capillary density derived with CapiAna was slightly higher as compared to the capillary density derived with the manual counting procedure. Nevertheless, we found no significant differences between these methods. Work is in progress to make detection on a frame-to-frame basis feasible. Secondly, optimal exposure is a prerequisite for a successful detection of the capillaries. Consequently, poor quality images (i.e., images with low contrast) need a higher extent of manual corrections. However, non-uniform intensity has only a limited impact, ensured by the use of a high-pass filter. Thirdly, out-of-focus effects occurring at the borders of the visual field may impair the automatic detection. Generally, the ROI was positioned in the center of the image, minimizing these effects. However, if the ROI could not be positioned optimally, out-of-focus capillaries could be included. This may generate false-negative detections. Yet, the detection turned out to be robust against these effects and only severe out-of-focus capillaries failed to be detected. Considering the limitations of these automatic detection steps, we concluded that manual correction of the detected capillaries is required.

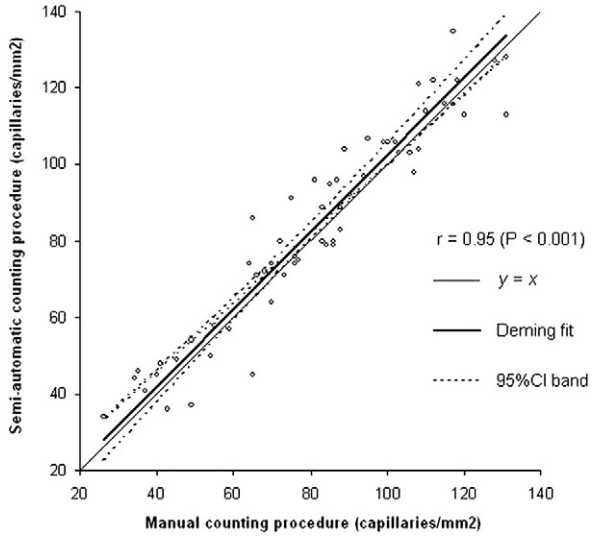

Fig. 6. Comparison of capillary densities between CapiAna (semi-automatic counting procedure) and the manual counting procedure by weighted Deming regression. Regression coefficient 1.01 (0.91; 1.10); intercept 1.75 (−6.04; 9.54).

The manual steps (i.e., selection of the frame range and positioning of the ROI and manual correction of detected capillaries) in CapiAna may introduce random errors and may therefore yield the largest contribution to the intra- and inter-observer variabilities. Nevertheless, CapiAna is a highly reproducible method. More precisely, CapiAna has a better reproducibility than the manual counting procedure; intra-observer CVs were 2.5% as compared to 3.2% and inter-observer CVs were 5.6% as compared to 7.2% (Jonk et al., 2011b). In addition, intra- and inter-observer CVs of CapiAna are better as compared to the CVs described in literature (4.5% and 10.1% respectively (Serne et al., 1999)). Thus, these data suggest that random errors in CapiAna are smaller than in the manual counting procedure.

CapiAna turned out to be an accurate method as compared to the manual counting procedure, i.e., there were no significant structural differences between the two methods. However, we only included twenty subjects for this study; therefore, a lack of power should be taken into consideration when interpreting these results. Nevertheless, the 95%CI of the mean difference – as demonstrated with the Bland–Altman analysis – has an acceptable range of approximately ±20%. In addition, we found no evidence for systematic errors between CapiAna and the manual counting procedure over the wide range of capillary densities studied. These observations strengthen the conclusion that CapiAna is in good agreement with the manual counting procedure. Hence, CapiAna can be used for a wide range of capillary densities and thus for the investigation of the skin microcirculation in health and disease.

CapiAna facilitates the use of skin capillaroscopy in microvascular research, since the method is shown to be equivalent to and interchangeable with the manual counting procedure with an intrinsically large reduction in analysis time. Microvascular dysfunction may constitute one of the links between insulin resistance and hypertension in the metabolic syndrome (Houben et al., 2012; Jonk et al., 2007; Muris et al., 2013). The skin is the only site available in humans allowing direct non-invasive visualization of capillaries at rest and during provocative stimuli. In addition, the cutaneous microcirculation is considered a representative vascular bed to examine the mechanism of generalized systemic microvascular dysfunction (Holowatz et al., 2008). Therefore, it is important to facilitate the use of skin capillaroscopy and with CapiAna this has become feasible.

In conclusion, we have developed a semi-automatic image analysis application, named CapiAna, for the assessment of skin capillary density, which is in agreement with the manual counting procedure, has a better reproducibility as compared to the classic manual counting procedure and is time-saving. As a result, skin capillaroscopy can be used in large-scale studies, which facilitate investigation of the microcirculation in health and disease.

Acknowledgments

We would like to thank Jean Scheijen and Amy Jonk for their technical support.

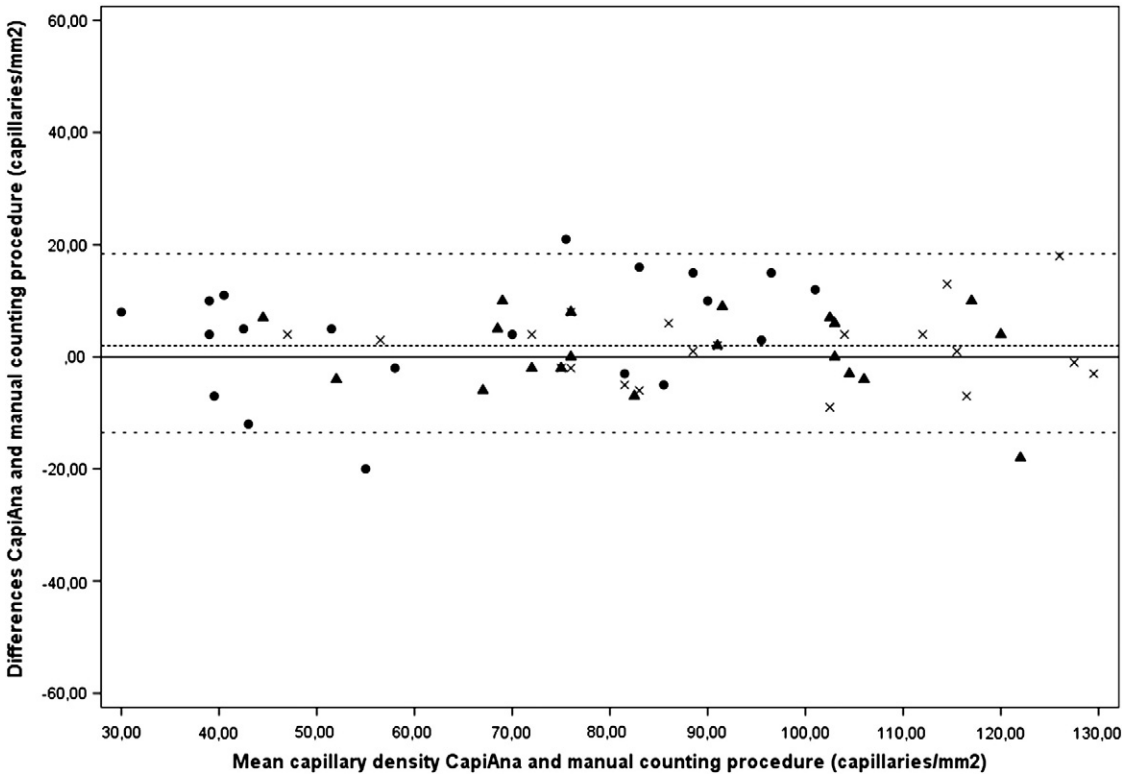

Fig. 7. Bland–Altman plot of the differences between CapiAna (semi-automatic counting procedure) and the manual counting procedure. ● baseline, ▲ hyperemic capillary recruitment, x venous congestion.

Table 2
Reproducibility of the semi-automatic image analysis application (CapiAna).

	Intra-observer variability	Inter-observer variability
	Coefficient of variation (%)	Coefficient of variation (%)
Baseline	3.5	6.6
Hyperemic (functional) capillary recruitment	1.7	5.4
Venous congestion	2.2	4.9
Overall	2.5	5.6

References

Bland, J.M., Altman, D.G., 1986. Statistical methods for assessing agreement between two methods of clinical measurement. Lancet 1, 307–310.

Clerk, L.H., Vincent, M.A., Jahn, L.A., et al., 2006. Obesity blunts insulin-mediated microvascular recruitment in human forearm muscle. Diabetes 55, 1436–1442.

de Jongh, R.T., Serne, E.H., Ijzerman, R.G., et al., 2004a. Free fatty acid levels modulate microvascular function: relevance for obesity-associated insulin resistance, hypertension, and microangiopathy. Diabetes 53, 2873–2882.

de Jongh, R.T., Serne, E.H., Ijzerman, R.G., 2004b. Impaired microvascular function in obesity: implications for obesity-associated microangiopathy, hypertension, and insulin resistance. Circulation 109, 2529–2535.

Giele, E.L., de Priester, J.A., Blom, J.A., et al., 2001. Movement correction of the kidney in dynamic MRI scans using FFT phase difference movement detection. J. Magn. Reson. Imaging 14, 741–749.

Holowatz, L.A., Thompson-Torgerson, C.S., Kenney, W.L., 2008. The human cutaneous circulation as a model of generalized microvascular function. J. Appl. Physiol. 105, 370–372.

Houben, A.J., Eringa, E.C., Jonk, A.M., et al., 2012. Perivascular fat and the microcirculation: relevance to insulin resistance, diabetes, and cardiovascular disease. Curr. Cardiovasc. Risk Rep. 6, 80–90.

Jonk, A.M., Houben, A.J., de Jongh, R.T., et al., 2007. Microvascular dysfunction in obesity: a potential mechanism in the pathogenesis of obesity-associated insulin resistance and hypertension. Physiology (Bethesda) 22, 252–260.

Jonk, A.M., Houben, A.J., Schaper, N.C., et al., 2010. Angiotensin II enhances insulin-stimulated whole-body glucose disposal but impairs insulin-induced capillary recruitment in healthy volunteers. J. Clin. Endocrinol. Metab. 95, 3901–3908.

Jonk, A.M., Houben, A.J., Schaper, N.C., et al., 2011a. Acute angiotensin II receptor blockade improves insulin-induced microvascular function in hypertensive individuals. Microvasc. Res. 82, 77–83.

Jonk, A.M., Houben, A.J., Schaper, N.C., et al., 2011b. Obesity is associated with impaired endothelial function in the postprandial state. Microvasc. Res. 82, 423–429.

Kubota, T., Kubota, N., Kumagai, H., et al., 2011. Impaired insulin signaling in endothelial cells reduces insulin-induced glucose uptake by skeletal muscle. Cell Metab. 13, 294–307.

Lang, C.H., 1992. Rates and tissue sites of noninsulin- and insulin-mediated glucose uptake in diabetic rats. Proc. Soc. Exp. Biol. Med. 199, 81–87.

Liu, Z., Liu, J., Jahn, L.A., et al., 2009. Infusing lipid raises plasma free fatty acids and induces insulin resistance in muscle microvasculature. J. Clin. Endocrinol. Metab. 94, 3543–3549.

Martin, R.F., 2000. General deming regression for estimating systematic bias and its confidence interval in method-comparison studies. Clin. Chem. 46, 100–104.

Meijer, R.I., de Boer, M.P., Groen, M.R., et al., 2012. Insulin-induced microvascular recruitment in skin and muscle are related and both are associated with whole body glucose uptake. Microcirculation 19, 494–500.

Muris, D.M., Houben, A.J., Schram, M.T., et al., 2013. Microvascular dysfunction: An emerging pathway in the pathogenesis of obesity-related insulin resistance. Rev. Endocr. Metab. Disord. 14, 29–38.

Press, W.H., Flannery, B.P., Teukolsky, S.A., et al., 1989. Numerical Recipes in C. Cambridge University Press, New York.

Serne, E.H., Stehouwer, C.D., ter Maaten, J.C., et al., 1999. Microvascular function relates to insulin sensitivity and blood pressure in normal subjects. Circulation 99, 896–902.

Serne, E.H., Ijzerman, R.G., Gans, R.O., et al., 2002. Direct evidence for insulin-induced capillary recruitment in skin of healthy subjects during physiological hyperinsulinemia. Diabetes 51, 1515–1522.

van Bussel, B.C., Ferreira, I., van de Waarenburg, M.P., et al., 2013. Multiple inflammatory biomarker detection in a prospective cohort study: a cross-validation between well-established single-biomarker techniques and an electrochemiluminescense-based multi-array platform. PLoS One 8, e58576.